Multisymbol QPSK Partitioning for Improved Frequency Offset Estimation of 16-QAM Signals

Ming Li, Jian Zhao, and Lian-Kuan Chen, *Senior Member, IEEE*

***Abstract*— We propose and investigate a generalized quadrature phase-shift keying (QPSK) partitioning algorithm for carrier frequency offset (CFO) estimation in coherent optical 16-quadrature amplitude modulation (QAM) receivers. The algorithm utilizes the phase difference between the samples with different time-domain separations, so that the estimation accuracy can be significantly enhanced. We propose a computationally efficient procedure to implement the generalized CFO estimation algorithm. In a 28-GBd coherent 16-QAM system, simulation results and complexity analysis show that the time span of 16 can realize an optimal balance between performance and complexity. With the optimal time span, the complexity to achieve a normalized variance of 10^{-8} for the CFO estimation error can be reduced by 150 times compared with the conventional QPSK partitioning algorithm.**

***Index Terms*— Carrier frequency offset estimation, coherent optical fiber communication, least-squares methods, quadrature amplitude modulation.**

I. Introduction

QUADRATURE amplitude modulation (QAM) in optical communication systems has recently attracted much attention in both academic and industrial fields. Compared with other modulation formats such as M-ary phase-shift keying (M-PSK), QAM may achieve higher spectral efficiency because of low optical signal-to-noise ratio (OSNR) requirement [1], [2]. In most digital coherent receivers, carrier frequency offset (CFO) estimation is required to alleviate the requirement of the wavelength alignment between the independently-running transmitter laser and the local oscillator (LO) [3]–[11]. Therefore, CFO estimation is essential for implementing digital coherent receivers using QAM signals.

Blind CFO estimation for QAM signals is more challenging than that for M-PSK signals, because the phases that represent data modulation are not equally spaced. Nevertheless, several techniques for blind CFO estimation for QAM signals have been proposed. For QAM signals, the CFO can be estimated by finding the argument that maximizes the periodogram of the fourth-powered samples [4], determining the argument that maximizes the periodogram of the phase of the samples after selective rotation [5], or finding the peak of the power spectrum of the samples when there is a residual carrier [6]. All these schemes involve fast Fourier transform (FFT) that consumes considerable memory and computation resources. The CFO can also be estimated by compensating the samples with different trial CFOs and select the trial CFO which minimizes the phase entropy of the compensated samples [7]. However, this method requires intensive computation as well. In order to reduce the computation complexity, a CFO estimation algorithm based on eighth-order statistics was proposed [8], but this algorithm requires a large number of samples to converge. In addition, the CFO can be estimated with low complexity by quaternary phase-shift keying (QPSK) partitioning, which only uses a subset of symbols that have phases similar to those in QPSK signals [9]. However, this algorithm also needs much more samples compared with that based on the periodogram of the fourth-powered samples.

The conventional QPSK partitioning algorithm only compares the phase difference between adjacent samples. It is expected that full utilization of correlation between samples with one or more symbols apart would improve the performance. The basic concept has been introduced in [12] and utilized in [10]. Similar idea can also be used to improve the receiver sensitivity for differential phase-shift keying signals [13] and in self-coherent detection [14], [15]. In this letter, we propose a generalized QPSK partitioning algorithm for 16-QAM signals based on this concept, and numerically show that multisymbol QPSK partitioning algorithm can significantly improve the estimation accuracy under a fixed number of estimation samples, or reduce the required number of samples for a given accuracy. We investigate the effect of phase noise on the number of time spans and propose a computationally-efficient procedure to implement the generalized QPSK partitioning algorithm. It is shown that an optimal balance between performance and complexity can be realized for a time span of 16, under which the generalized algorithm can reduce the complexity by 150 times, compared to that of the conventional QPSK partitioning algorithm, for the same estimation accuracy. The proposed algorithm can also be extended to higher-level formats such as 64 QAM.

II. The Proposed CFO Estimation Algorithm

In the conventional QPSK partitioning algorithm for 16-QAM signals, the CFO f_c can be estimated as [9]

$$\hat{f}_c = \frac{1}{8\pi T} \arg\left(\sum_{n=1}^{N-1} w(n, n+1) S_{n+1}^4 (S_n^4)^* \right), \qquad (1)$$

Manuscript received August 15, 2014; revised September 15, 2014; accepted September 17, 2014. Date of publication September 23, 2014; date of current version December 4, 2014. This work was supported in part by the Science Foundation Ireland under Grant 11/SIRG/I2124 and Grant 13/TIDA/I2718, in part by the Irish Research Council for Science, Engineering and Technology through the New Foundations 2013 CDAMT, in part by Hong Kong Research Grants Council under Direct Grant for Research, and in part by the University Grant Committee of HKSAR under Grant AoE/E-02/08.

M. Li is with the Institute of Network Coding, Chinese University of Hong Kong, Hong Kong (e-mail: mingli@inc.cuhk.edu.hk).

J. Zhao is with the Tyndall National Institute, University College Cork, Cork, Ireland (e-mail: jian.zhao@tyndall.ie).

L.-K. Chen is with the Department of Information Engineering, Chinese University of Hong Kong, Hong Kong (e-mail: lkchen@ie.cuhk.edu.hk).

Digital Object Identifier 10.1109/LPT.2014.2359735

where S_n is the n^{th} received sample, $w(n_1, n_2)$ is one when both S_{n1} and S_{n2} are identified as class-I symbols as defined in [9] and is zero otherwise, T and N are the symbol duration and the number of samples for CFO estimation, arg(•) is the argument function, respectively. The conventional QPSK partitioning algorithm uses the metric

$$\varphi(1) = \arg\left(\sum_{n=1}^{N-1} w(n, n+1) S_{n+1}^4 (S_n^4)^*\right) \tag{2}$$

as an estimate of $8\pi f_c T$. Since only a subset of sample pairs are employed, it requires large number of samples to converge. To make full use of the correlation information, we calculate multisymbol metrics:

$$\varphi(m) = \arg\left(\sum_{n=1}^{N-m} w(n, n+m) S_{n+m}^4 (S_n^4)^*\right), \tag{3}$$

where $m = 1, 2, \ldots, M$. Then

$$\begin{cases} \varphi(1) \equiv 1 \times 8\pi f_c T + \varepsilon_1 \\ \varphi(2) \equiv 2 \times 8\pi f_c T + \varepsilon_2 \\ \quad \bullet \quad \bullet \quad \bullet \\ \varphi(M) \equiv M \times 8\pi f_c T + \varepsilon_M \end{cases} (\text{mod } 2\pi), \tag{4}$$

where ε_m is the random error term for $\varphi(m)$. Because $\varphi(m)$ depends linearly on f_c only when $|8\pi m f_c T| < \pi, m = 1, 2, \ldots, M$, the CFO estimation range based on each individual $\varphi(m)$ is $(-1/(8mT), 1/(8mT))$. However, we may firstly have a coarse estimation of the CFO using $\varphi(1)$, which has the widest estimation range but the highest sensitivity to the noise. Then according to the obtained information, unwrap $\varphi(2)$ by adding multiples of 2π to make the estimation range based on $\varphi(2)$ match that based on $\varphi(1)$. We continue this operation until $\varphi(M)$ is unwrapped. Consequently, the CFO estimation range based on the resulting unwrapped phases, represented by $\Phi(1)$, $\Phi(2), \ldots, \Phi(M)$, can be extended to $(-1/(8T), 1/(8T))$. From (4), the noise impact on the estimated f_c using $\Phi(m)$ is $1/m$ times of that using $\Phi(1)$. Therefore, in order to optimally combine the information in (4), f_c can be estimated by setting the partial derivative of the summed squared error with respect to f_c to zero

$$\partial \sum_{m=1}^{M} |\Phi(m) - 8\pi m f_c T|^2 / \partial f_c = 0. \tag{5}$$

The estimated f_c can be represented by weighted sum of $\Phi(m)$ as:

$$\hat{f}_c = \sum_{m=1}^{M} m\Phi(m) / (8\pi T \sum_{m=1}^{M} m^2) \tag{6}$$

III. Simulation Setup and Results

The performance of the proposed CFO estimation algorithm was evaluated by simulation. The modulation format of the optical signal was 16-QAM and the baud rate was 28 GBd. The phases of the transmitter laser and the optical LO were modeled as a Wiener process to account for their finite laser linewidth $\Delta\nu$. Additive white Gaussian noise was added to adjust the OSNR. A 2^{nd}-order Gaussian optical band-pass filter was used to filter out the out-of-band amplified spontaneous emission noise before the signal was coherently detected. The receiver electrical response had 5^{th}-order Bessel characteristics with a 3-dB bandwidth of 24 GHz. Then the electrical signal was sampled at a sampling rate of two samples per symbol and equalized using a 9-tap feed-forward equalizer. The tap weights were updated by the decision-adjusted modulus algorithm [16]. The output of the equalizer was then utilized for CFO estimation. For determining the mean and the variance of the CFO estimation error, 1000 rounds of simulation were performed.

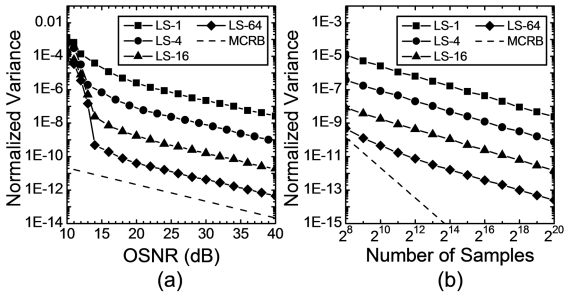

Fig. 1. Normalized variance of the CFO estimation error and the MCRB as (a) functions of OSNR when 1024 samples are used for the CFO estimation, and (b) functions of number of samples utilized at 20-dB OSNR. For (a) and (b), the CFO is 2 GHz and the laser linewidth is 0 kHz.

Fig. 1(a) shows the variance of the CFO estimation error as functions of OSNR for the proposed algorithm. The variance is normalized by multiplying it with the squared symbol duration T. The algorithms utilizing different numbers of time spans – the value of M in (6) – are denoted by LS-1, LS-4, LS-16, and LS-64. LS-1 represents the conventional QPSK partitioning algorithm for 16-QAM signals. For reference, we also plot the modified Cramér-Rao bound [17] denoted by MCRB and calculated as

$$\text{MCRB}(\hat{f}_c T) = \frac{3}{2\pi^2 N^3} \times \frac{1}{\text{SNR}}, \tag{7}$$

where SNR is the signal-to-noise ratio for the samples. The laser linewidth and the CFO are set to be zero and 2 GHz, respectively. 1024 samples are utilized for CFO estimation. For all algorithms with different number of time spans, the normalized variances drop as the OSNR increases. When only one time span is used (the conventional QPSK partitioning algorithm), the performance is far from the MCRB. As the number of time spans increases to four, the normalized variance for LS-4, $\sigma^2_{\text{LS}-4}$, is reduced by more than one order of magnitude, verifying the effectiveness of the proposed algorithm. This trend continues as the number of time spans further increases to 16 and 64. It is expected that the performance will gradually approach the theoretical limit when the number of spans further increases. However, the complexity and sensitivity to phase noise will also increase. Fig. 1(b) shows the normalized variance versus the number of samples utilized for CFO estimation. It is confirmed that LS-4/16/64 can achieve better estimation accuracy than LS-1 under a fixed number of samples utilized and OSNR value. More importantly, we can see that for a fixed estimation accuracy,

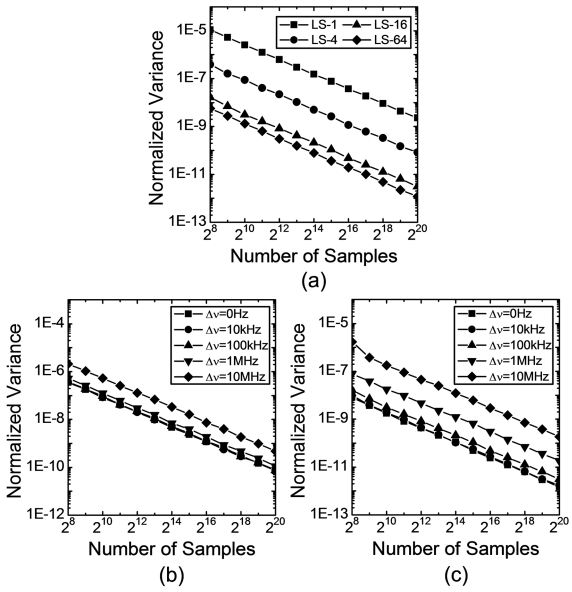

Fig. 2. (a) Normalized variance of the CFO estimation error as functions of number of samples used with different algorithms when the laser linewidth is 100 kHz; normalized variance of the CFO estimation error as functions of number of samples utilized (b) for LS-4 and (c) for LS-16 with different laser linewidths. For (a)–(c), the CFO is 2 GHz and the OSNR is 20 dB.

the proposed algorithm can significantly reduce the required number of samples. Under a normalized variance σ^2 of 10^{-8} at 20-dB OSNR, the required number of samples for LS-16 is reduced by ∼660 times compared to that required by LS-1. Note that although the value of σ^2 increases as the OSNR decreases, for a system that can achieve σ^2 of 10^{-8} at 20-dB OSNR, high estimation accuracy can still be ensured for the whole OSNR range of interest for a 28-GBd 16-QAM signal (typically OSNR $>$ 15 dB), resulting in negligible penalty (with respect to the case CFO $=$ 0 GHz, w/o CFO estimation) as will be shown in Fig. 3(b).

The use of phase correlation between samples with one or more symbols apart would place more stringent requirement on the laser phase noise. Fig. 2(a) re-plots the normalized variance of the CFO estimation error versus the number of samples for a laser linewidth of 100 kHz. Comparison with Fig. 1(b) shows that LS-1, LS-4, and LS-16 have similar performance when the laser linewidth increases from 0 to 100 kHz. In contrast, the benefit of using LS-64 vanishes for 100-kHz laser linewidth (taking the complexity as will be discussed later into consideration). To address this issue more clearly, Fig. 2(b) and Fig. 2(c) show the performance of LS-4 and LS-16 under different laser linewidths when the CFO is 2 GHz. It can be seen that the performance of both LS-4 and LS-16 degrades as the laser linewidth increases. LS-4 is more tolerable to phase noise with negligible penalty under 100-kHz linewidth (a value widely used in practical coherent systems). On the other hand, slight performance degradation is observed for LS-16 when the laser linewidth increases from 0 to 100 kHz. However, LS-16 is still a near-optimal solution due to its better absolute performance than LS-4.

To further investigate the performance of LS-16, bit error rate (BER) performance is illustrated in Fig. 3. Note that the

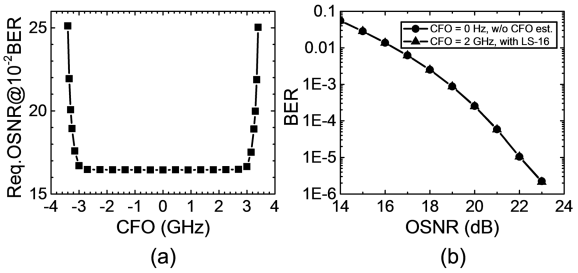

Fig. 3. (a) Required OSNR for a BER of 10^{-2} for LS-16 as a function of the CFO; (b) BER as functions of OSNR for the case without CFO and CFO estimation, and for the case with 2-GHz CFO and LS-16 for CFO estimation. 1024 samples are used and the laser linewidth is 100 kHz.

influence of the residual CFO error on the BER performance may depend on the carrier phase estimation method. In the figure, we used blind phase search algorithm [18], with 16 branches of trial phases and 17-point moving average for smoothing the errors. The linewidth of the lasers is 100 kHz. Fig. 3(a) shows the required OSNR at a BER of 10^{-2} versus the CFO. It can be seen that the variation in the required OSNR is $<$0.5 dB when the CFO is between -3.05 GHz and 3.05 GHz. Beyond $\pm$3.05 GHz, the OSNR penalty increases abruptly. The CFO estimation range is around $(-1/(8T), 1/(8T))$, as stated in Section II. Fig. 3(b) shows the BER versus the OSNR for LS-16 at 2-GHz CFO, and for the case without CFO and CFO estimation. The number of samples utilized by LS-16 for CFO estimation is chosen to approximately achieve σ^2 of 10^{-8} at 20-dB OSNR. The BER curve with 2-GHz CFO and LS-16 for CFO estimation coincides with that for the case when the CFO is zero and CFO estimation is not used. Therefore, LS-16 can accurately estimate the CFO and the penalty brought about by the CFO is negligible.

IV. Complexity Analysis

In this letter, we propose the following computation procedure to minimize the implementation complexity of the proposed scheme. In the calculation, we neglect the boundary effect that has negligible effect for a large N. The basic idea behind this procedure is that in (3), S_n^4 is required to be calculated only once for any $w(n, n+m) \neq 0$ or $w(n-m, n) \neq 0$ with any m that satisfies $1 \leq m \leq M$. Assuming the number of samples used for CFO estimation is N, we will calculate the required number of real multiplications for the following five parts. 1) The squared amplitude of the samples for identifying class-I samples as defined in [9]: This needs two real multiplications for each sample, resulting in $2N$ total real multiplications. 2) Fourth power of the class-I samples that has at least one class-I sample in the M preceding or M succeeding samples: The expected number of such samples is $\sim(1/2) \times (1 - (1/2)^{2M}) \times N$, and each such sample requires four additional real multiplications. Therefore, the expected total number of real multiplications required in this part is $\sim 3N/2$ for LS-1 and $\sim 2N$ for LS-4/16/64. 3) Product of fourth-powered class-I sample with the conjugate of any fourth-powered class-I sample that is within preceding M samples: The expected number of products for

TABLE I
COMPLEXITY ANALYSIS OF LS-1/4/16/64 TO ACHIEVE A NORMALIZED VARIANCE OF 10^{-8} UNDER 100-kHz LASER LINEWIDTH

	LS-1	LS-4	LS-16	LS-64
Required N	$\sim 2.4\times10^5$	$\sim 8.6\times10^3$	$\sim 3.6\times10^2$	$\sim 1.4\times10^2$
Required number of real multiplications for a fixed N	$\sim 9N/2$	$\sim 8N$	$\sim 20N$	$\sim 68N$
Required number of real multiplications	$\sim 1.1\times10^6$	$\sim 6.9\times10^4$	$\sim 7.2\times10^3$	$\sim 9.4\times10^3$

each sample is $\sim(1/4) \times M$ and the expected number of products for all samples is $MN/4$. Each product requires four real multiplications so the expected required number of real multiplications in this part is MN. 4) Unwrapping $\varphi(1)$, $\varphi(2), \ldots, \varphi(M)$: This operation requires only comparison and addition without real multiplication. 5) The weighted sum of $\Phi(m)$ using (6): It requires M real multiplications, but this is generally much smaller than that for parts 1-3 and thus can be neglected. Based on this computation, the number of real multiplications for LS-1 and LS-M are $\sim 9N/2$ and $\sim(M+4)N$, respectively.

Table I compares the required number of real multiplications for LS-1/4/16/64 to achieve a normalized variance of 10^{-8} at 20-dB OSNR for a 100-kHz laser linewidth. It can be seen that compared with LS-4 (or LS-16), LS-1 requires around 28 (or 660) times of N to achieve the same accuracy. Due to the higher sensitivity to laser linewidth, further increasing the number of time spans to 64 does not show significant reduction in N (only by an additional 2.6 times) compared to LS-16, for a 100-kHz laser linewidth. On the other hand, for a fixed N, the required number of real multiplications for LS-4/16/64 is approximately 1.8, 4.4, and 15.1 times of that for LS-1. Consequently, from the last row of Table I, it can be concluded that the time span of 16 is optimal and LS-16 can reduce the required number of real multiplications by a factor of 150 to realize a normalized variance of 10^{-8}. This verifies the advantages of the proposed algorithm over conventional QPSK partitioning algorithm.

V. CONCLUSION

We have proposed and investigated a generalized QPSK partitioning algorithm to enhance the performance of the conventional QPSK partitioning algorithm in coherent optical 16-QAM receivers. The proposed algorithm uses the phase difference between samples with different time-domain separations. We have investigated the performance sensitivity to phase noise for different utilized time spans and proposed a computationally-efficient procedure to implement the generalized algorithm. Simulation results and complexity analysis show that with a 100-kHz laser linewidth, LS-16 can realize an optimal balance between performance and complexity under a normalized variance of 10^{-8} for the CFO estimation error, under which the complexity can be reduced by 150 times, compared to the conventional QPSK partitioning algorithm. The proposed CFO estimation algorithm can be implemented in burst-mode coherent optical 16-QAM receivers in which the efficiency, in terms of both the number of samples and the hardware resources required, is important.

REFERENCES

[1] P. J. Winzer, A. H. Gnauck, C. R. Doerr, M. Magarini, and L. L. Buhl, "Spectrally efficient long-haul optical networking using 112-Gb/s polarization-multiplexed 16-QAM," *J. Lightw. Technol.*, vol. 28, no. 4, pp. 547–556, Feb. 15, 2010.

[2] M. Nakazawa, S. Okamoto, T. Omiya, K. Kasai, and M. Yoshida, "256-QAM (64 Gb/s) coherent optical transmission over 160 km with an optical bandwidth of 5.4 GHz," *IEEE Photon. Technol. Lett.*, vol. 22, no. 3, pp. 185–187, Feb. 1, 2010.

[3] A. Leven, N. Kaneda, U.-V. Koc, and Y.-K. Chen, "Frequency estimation in intradyne reception," *IEEE Photon. Technol. Lett.*, vol. 19, no. 6, pp. 366–368, Mar. 15, 2007.

[4] M. Selmi, Y. Jaouën, and P. Ciblat, "Accurate digital frequency offset estimator for coherent PolMux QAM transmission systems," in *Proc. 35th ECOC*, Sep. 2009, pp. 1–2, paper P3.08.

[5] Y. Cao, S. Yu, Y. Chen, Y. Gao, W. Gu, and Y. Ji, "Modified frequency and phase estimation for M-QAM optical coherent detection," in *Proc. 36th ECOC*, Sep. 2010, pp. 1–2, paper We.7.A.1.

[6] Y. Gao, A. P. T. Lau, and C. Lu, "Residual carrier-aided frequency offset estimation for square 16-QAM systems," in *Proc. 18th Int. Conf. OECC/PS*, Jul. 2013, pp. 1–2, paper TuPR-8.

[7] S. Dris, I. Lazarou, P. Bakopoulos, and H. Avramopoulos, "Frequency offset estimation in M-QAM coherent optical systems using phase entropy," in *Proc. CLEO*, May 2012, pp. 1–2, paper CF1F.2.

[8] M. Li and L.-K. Chen, "Blind carrier frequency offset estimation based on eighth-order statistics for coherent optical QAM systems," *IEEE Photon. Technol. Lett.*, vol. 23, no. 21, pp. 1612–1614, Nov. 1, 2011.

[9] I. Fatadin and S. J. Savory, "Compensation of frequency offset for 16-QAM optical coherent systems using QPSK partitioning," *IEEE Photon. Technol. Lett.*, vol. 23, no. 17, pp. 1246–1248, Sep. 1, 2011.

[10] D. Huang, T.-H. Cheng, and C. Yu, "Accurate two-stage frequency offset estimation for coherent optical systems," *IEEE Photon. Technol. Lett.*, vol. 25, no. 2, pp. 179–182, Jan. 15, 2013.

[11] M. Li, J. Zhao, and L.-K. Chen, "Least-squares carrier frequency offset estimation for coherent optical QPSK receivers," presented at the CSNDSP, 2014.

[12] M. Morelli and U. Mengali, "Feedforward frequency estimation for PSK: A tutorial review," *Eur. Trans. Telecommun.*, vol. 9, no. 2, pp. 103–116, Mar./Apr. 1998.

[13] J. Zhao and L.-K. Chen, "Three-chip differential phase-shift keying maximum likelihood sequence estimation for chromatic-dispersion and polarization-mode-dispersion compensation," *Opt. Lett.*, vol. 32, no. 12, pp. 1746–1748, Jun. 2007.

[14] J. Zhao, M. E. McCarthy, and A. D. Ellis, "Electronic dispersion compensation using full optical-field reconstruction in 10 Gbit/s OOK based systems," *Opt. Exp.*, vol. 16, no. 20, pp. 15353–15365, Sep. 2008.

[15] M. Nazarathy, X. Liu, L. Christen, Y. K. Lize, and A. E. Willner, "Self-coherent multisymbol detection of optical differential phase-shift keying," *J. Lightw. Technol.*, vol. 26, no. 13, pp. 1921–1934, Jul. 1, 2008.

[16] W. A. Sethares, G. A. Rey, and C. R. Johnson, "Approaches to blind equalization of signals with multiple modulus," in *Proc. ICASSP*, vol. 2. May 1989, pp. 972–975, paper D3.21.

[17] A. N. D'Andrea, U. Mengali, and R. Reggiannini, "The modified Cramer–Rao bound and its application to synchronization problems," *IEEE Trans. Commun.*, vol. 42, no. 234, pp. 1391–1399, Feb./Apr. 1994.

[18] T. Pfau, S. Hoffmann, and R. Noé, "Hardware-efficient coherent digital receiver concept with feedforward carrier recovery for M-QAM constellations," *J. Lightw. Technol.*, vol. 27, no. 8, pp. 989–999, Apr. 15, 2009.